The Open-Access Journal for the Basic Principles of Diffusion Theory, Experiment and Application

CONCENTRATION DEPENDENT DIFFUSIVITIES OF MODEL SOLVENTS IN HEAVY OIL

Vijitha Mohan [1], P. Neogi[1], Baojun Bai [2]

[1] Department of Chemical and Biochemical Engineering

[2] Geosciences and Geological and Petroleum Engineering

Missouri University of Science and Technology, Missouri, USA

Corresponding author: Parthasakha Neogi, Dept. of Chemical and Biochemical Engineering, Missouri University of Science and Technology, Rolla, Missouri 65409-1203, USA.
E-mail: neogi@mst.edu , Tel: (573) 341-4460.

Keywords

Concentration-dependent diffusivity; light hydrocarbons in heavy oil; dissolution-desorption; mass transfer with sharp interfaces; high viscosities; low diffusivities

Abstract

The rates of dissolution of heavy crude oil in liquid solvents and rates of desorption of solvents from oil have been measured. The crude oil used is a non-volatile heavy oil of 4253 mPa.s viscosity at room temperature. The solvents used are hexane, heptane and toluene. When the oil (black) is contacted with a solvent (transparent) an interface is seen which moves with

time and takes a very long time to become fuzzy. The rate of movement of the front is measured. The dissolution experiments give very consistent results, but there are two parameters involved, D_o, the diffusivity at infinite dilution and α which determines the concentration dependence. As a result it is necessary to do desorption experiments to be able to calculate both constants from the rate of movement of the front data. However, desorption experiments could not be performed under conditions of low concentrations suitable for the present case because of the very viscous nature of the oil. As a result, although the desorption experiments also showed good results, they could not be used to obtain good values of the parameters. When Stokes-Einstein equation was used to calculate D_o, excellent results were obtained with $\alpha \sim 10$ for the dissolution experiments and good deal smaller for the desorption experiments. That result is used to conclude that the above form for concentration dependent diffusivity is correct and concentration dependence is very high at low solvent concentrations explaining the sharp interfaces during dissolution. Other evidences have also been offered.

1. Introduction

Heavy oil extraction offers challenges because of its high viscosity (above 100 cp). One process introduces steam at high temperature and pressure over oil in the reservoir. The steam heats up the oil and the viscosity drops to 1 cp, which helps to bring up the oil to the surface which is the steam assisted gravity drainage (SAGD). In a related process n-hexane, n-heptane vapors are used to treat the oil. They dilute the oil bringing down the viscosity. The decrease in viscosity is effected by dilution with solvent and not through heat as in steam driven recovery. In addition, asphaltenes are precipitated which lowers the viscosity further. It is called the solvent vapor extraction (VAPEX) process. An overview of this area is presented by Banerjee [1] and a quantitative description of VAPEX, but without mass transfer, has been given by Lin et al [2]. Although the solvents are introduced in vapor form, when dissolved in oil they acquire consistency of liquid state, that is, condensed phase [3]. This holds even when the solvent is a permanent gas. As a result in the work below liquid phase solvents are used to look at diffusivities of solvents in oil.

1.1. Self – sharpening

We are interested here in quantifying the rate of dissolution of heavy oil in C_6, C_7 and toluene. A small amount of heavy oil is put in a test tube and a solvent is layered over it. Under conditions of no stirring, an interface is seen. The location of the interface moves with time till the solvent turns brown to black and nothing else can be observed. The question arises as to why an interface should exist when the oil and solvent are miscible. To answer this question (and subsequently) we assume that the heavy oil is very much like a polymer. In such a case a look at the rate of dissolution of polymer in a solvent also shows that an interface forms [4] and stays for a long time. The plane of color or refractive index contrast in non-equilibrium conditions is located using material balances exactly as in an equilibrium liquid-liquid interface, as shown subsequently. We, therefore refer to it as an interface here. There are explanations as to why this happens, but the one we are interested is in the role of concentration dependent diffusivity [5]. The profile of penetrant entering the oil is sketched in Fig. 1(a). The diffusivity is strongly concentration dependent and here taken to be

$$D = D_o e^{\alpha\phi} \tag{1}$$

where $\alpha\phi$ is positive and large ~ 5-15, α is defined in Eq. (1) and ϕ is the volume fraction of the penetrant. D_o is the diffusivity at infinite dilution. As mentioned below, Eq. (1) is based on form of molecular theory which is called the free volume theory. We look at its approximate expression for diffusivity at high dilution which forms the rate limiting step. More details on both are given below in section 1.2. Now, the regions of large concentrations will show higher fluxes than the region of lower concentrations which will show lower fluxes. This makes the profile become sharper as shown in Fig. 1(b). An interface is now observable. For diffusivity given by Eq. (1), Neogi [6] has obtained the profile which is shown in Fig. 1(c) for $\alpha\phi_\infty$ = 15. Note that the penetration of the solvent is limited by the region of low solvent concentration which moves the slowest. It is important to note that ends do not matter in Figs. 1(b) and 1(c), but is all important in Fig. 1(a). Thus, it is possible to take the results of Neogi [6] for a membrane with a finite thickness and transfer it to an infinite system in the contacting process described earlier. It is noteworthy, that some of the boundary conditions in contacting are effectively at infinite distances.

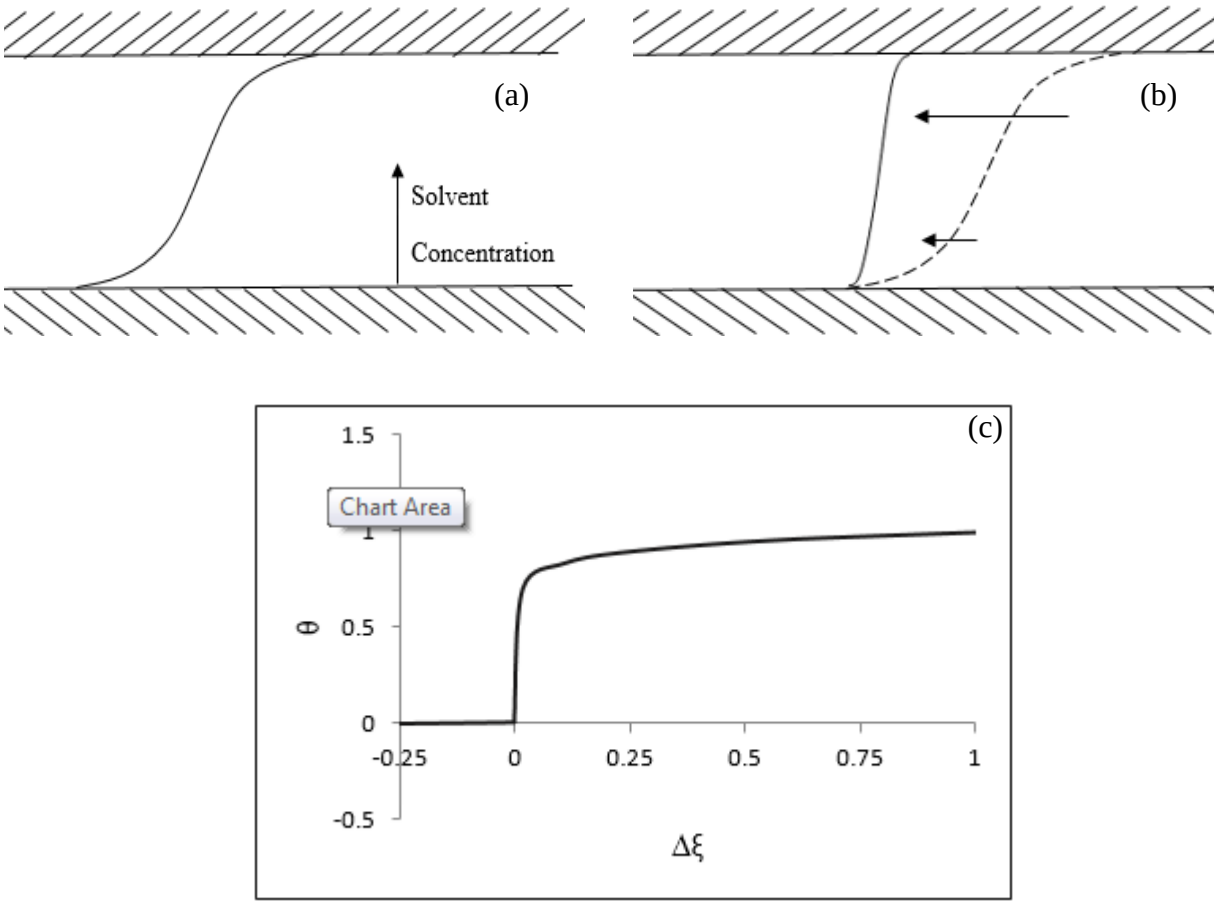

Fig. 1: (a) Schematics of penetrant entering the oil under diffusion when the diffusivity is a constant. The concentration profile is smooth. (b) If the diffusivity is an increasing function of the solvent concentration then the region of the profile with higher concentration moves ahead much faster than the basic profile and the region of low concentration more slowly. The consequence is a buildup, also called self-sharpening. (c) Neogi's [6] solution to Eqs. (1) and (7) plotted in the form of dimensionless concentration, θ and dimensionless distance, $\Delta\xi$ from the interface for $\alpha\phi_\infty = 15$. The foot of the profile is not discontinuous and it is easy to see where the interface between oil (black) and solvent (transparent) will be.

1.2. Diffusion coefficient, flux and conservation equation

The diffusivity of a penetrant in a polymer is given by free volume theory [7] as

$$D = RTA_d.\exp[-\frac{B_d}{f+(g-f)\phi}] \qquad (2)$$

where A_d and B_d are constants, and B_d is the size of a hole that needs to be created for the penetrant to move into. It is a molecular theory started by Cohen and Turnbull [8] that works when the free volumes are small and controls molecular movement. More recently, Sabbagh and Eu [9] have produced a perturbation expansion that provides a second term to the result of Cohen and Turnbull [8] which additions have not been used here as the molecular weight of oil is needed. The volume fraction of the penetrant is ϕ, and f and g are the free volume fractions of the polymer and the penetrant. Free volume is defined as the total volume less the volume occupied by molecules of hard dimensions. The free volume fraction of a polymer f is small but that of small penetrant species g is large, as a result the free volume increases with solvent concentration and so does the diffusivity. Fujita [10] has reviewed this area earlier and showed that other properties also follow the free volume theory. Tran et al [11] fitted the data of Chung et al [12] of a heavy oil (Bartlett crude), with and without CO_2. Isothermal compressibility, coefficient of volumetric expansion, swelling by CO_2 and viscosity data were used to predict the constants A_μ and B_μ, as well as the free volume f as a function of temperature and pressure; where viscosity is given by

$$\mu = RTA_\mu . \exp[\frac{B_\mu}{f + (g - f)\phi}] \qquad (3)$$

Here, $B_\mu \sim B_d \sim 1$. Thus, D and μ have an inverse relationship. The free volume of CO_2 was found to be independent of pressure but strongly dependent on temperature. Using these, Tran et al [11] were able to predict the remaining viscosity data without any additional parameters. Chung et al [12] did not have any data on diffusivity and Tran et al [11] predicted those in form of D/D_o as a function of ϕ using Eq. (2). It resembled closely Eq. (1) with $\alpha\phi_\infty \sim 10$. It follows that the free volume theory works well for heavy oil, because the free volume of heavy oil is low and rate limiting. When the free volume becomes large, as at very high temperatures, Arrhenius type of activation energy controls the mobility. We have begun to explore by how much we can apply free volume theory to heavy oil, and the results so far look good. On the other hand there is a large volume of successful application to polymer systems by Vrentas and Duda [7] and Fujita [10].

More specifically, Tran et al [11] found f to be larger in heavy oils than observed in polymers (but still small), thus $(g - f)$ is smaller (but still larger than f). We can obtain diffusivity at infinite dilution from Eq. (2) and on dividing one by the other get

$$D / D_o = \exp[\frac{B_d (g - f)\phi}{f(f + (g - f)\phi)}] \tag{4a}$$

which becomes for small values of ϕ,

$$D / D_o = \exp[\frac{B_d (g - f)\phi}{f^2}] \tag{4b}$$

and thus

$$\alpha = B_d (g - f) / f^2 \tag{4c}$$

Note that Eq. (4c) shows α in Eq. (1) to be positive [13] and large because f^2 is smaller than $(g - f)$. Tran et al [11] found for CO_2 in Bartlett heavy oil that $(g - f) \sim 3f$, so that α for them is $\sim 3/f$ and the smallest value of $f \sim 0.02$.

There is yet another reason for using a volume based theory for diffusivity. There are good many methods for breaking down heavy oils into individual components or groups, with specific or average molecular weights. However, considerable differences exist in the results for average molecular weights for the same oil [1]. Consequently, it is best to move to volumes based on volumes/volume fractions and take oil to be a single pseudocomponent. It is worked well earlier [11, 14] and works well here as seen below.

In the present case Fig. 2(a) shows that the total volume of oil and solvent does not change with time. Consequently, we assume that the partial volumes of oil and solvent remain constant and same as those of pure components. In a one dimensional system, this has an important result that when we use volume average velocity to determine the fluxes, there is no convective term [15] that is otherwise expected [16]. The flux in the stationary coordinates is same as that given by Fick's law in moving coordinates

$$N_x = J_x \tag{5}$$

following notations in Bird, et al [17]. If a volume average velocity is used for Fick's law, it results in

$$J_x = -D\frac{\partial c}{\partial x} \tag{6}$$

exactly. This leads to conservation equation

$$\frac{\partial c}{\partial t} = -\frac{\partial N_x}{\partial x} = \frac{\partial}{\partial x} D\frac{\partial c}{\partial x} \tag{7}$$

When volumes are additive, the specific molar volume v^o remains a constant and same as that of the pure system. Hence multiplying Eq. (7) with v^o leads to

$$\frac{\partial \phi}{\partial t} = \frac{\partial}{\partial x} D\frac{\partial \phi}{\partial x} \tag{8}$$

We have taken time to develop the conservation equation in this system as discussions have become very contentious in this area [18].

1.3. Approximate concentration profile of the solvent

Solution to Eqs. (1) and (8) when $\alpha\phi$ is large is difficult to obtain. Neogi [6] assumed that $\alpha\phi_\infty = \bar{\alpha} = \ln\left|\frac{1}{\varepsilon}\right|$ where ϕ_∞ is the saturation volume fraction of the solvent and ε is a small quantity. When $\bar{\alpha}$ = 5, ε = 7x10^{-3} and when $\bar{\alpha}$ = 15, ε = 3x10^{-7}. Such an assumption led Neogi [6] for the problem of diffusion in a membrane to an asymptotic solution for $\theta = \phi/\phi_\infty$ where the membrane initially has no solvent. The profile obtained is very sharp as shown in Fig. 1(c) and rides on a pseudo-interface between the solvent-rich and solvent lean regions. The boundary conditions are θ goes to zero or 1, as x goes to minus or plus infinity. Dimensionless quantity ξ_o was defined as current location of an interface in the membrane, dividing a region which is saturated by the solvent, θ = 1, from a region which is completely dry, θ = 0. The overall mass of solvent is conserved. In dimensional form the location of this interface changes as

$$\Delta x_o = \left[\frac{2D_o e^{\alpha\phi_\infty} t}{\alpha\phi_\infty}\right]^{1/2} \tag{9}$$

where x_o is the dimensional ξ_o and Δx_o is the amount by which the interface has moved. Since this is the quantity that we measure experimentally, comparing the measurements to theory becomes very easy. Eq. (9) contains a problem in the limit α goes to zero, because it has been obtained under the condition that α is large. An empirical correction would be

$$\Delta x_o = [\frac{2D_o(e^{\alpha\phi_\infty} - 1)t}{\alpha\phi_\infty}]^{1/2} \tag{10}$$

where the exponential factor is much larger than 1 for large values of α. With this minor change, Eq. (10) predicts that if α is zero, the diffusivity predicted by both Eqs. (10) and (1) is D_o. If the initial concentration of the solvent in oil is ϕ_o instead of zero, we get

$$\Delta x_o = [\frac{2D_o(e^{\alpha\phi_\infty} - 1)t}{\alpha(\phi_\infty - \phi_o)}]^{1/2} \tag{11}$$

where the above correction for small values of α has been made. Usually, $\phi_\infty = 1$.

When oil is contacted with a solvent some discussion is needed on how the above results can be applied. As shown in Fig. 2(a) a visible interface or pseudo-interface is observed for a long time even though some mass transfer is going on as evidenced by the swelling of the oil phase. The oil phase is black and the solvent phase is transparent. It is also possible to define a mathematical interface with ϕ = 1 on one side and ϕ = 0 on the other such that the solvent material balance is satisfied $\int_0^L \phi dx = 1.(L - x_o) + 0.x_o$ where zero and L are the two boundaries. It is evident from Fig. 1(c) that this mathematical interface will lie very close to the region where the solvent concentration changes very sharply, which is the region of visible interface. If the visual interface can be located by color change within a band of Δ in its location, then it can also be assumed that the mathematical interface x_o will lie there with an error of $\pm$ $\Delta/2$. Then the above equations will apply with this error. Thus, it is being assumed that the mathematical interface also lies in this band. At very large times not just this band becomes large, the solvent becomes brown when it becomes difficult to identify the region of transition.

In desorption experiments, vacuum is pulled over oil containing solvent. The result for desorption is

$$\Delta x_1 = \left[2\frac{e^{\hat{\alpha}}(e^{\hat{\alpha}} - 1)}{\hat{\alpha}} D_o t \right]^{1/2} \tag{12}$$

where x_1 is the location of the mathematical interface and $\hat{\alpha} = \alpha\phi_o$. However, both the interfaces, mathematical and pseudo-interface, between solvent rich ($\phi = \phi_o$) - solvent lean ($\phi = 0$) regions, lie inside the oil which is black. Thus the visual interface cannot be observed. There is a third interface here, the liquid-vacuum interface. As the volumes are additive, the total change in volume leads to

$$\Delta x_i = \phi_o \Delta x_1 = \phi_o \left[2\frac{e^{\hat{\alpha}}(e^{\hat{\alpha}} - 1)}{\hat{\alpha}} D_o t \right]^{1/2} \tag{13}$$

where x_i here is the oil-vacuum interface, where 1 has been subtracted off to prevent singularity at $\hat{\alpha} = 0$.

In the experiments described below, we measure the rate at which a sharp interface between the oil rich region and the solvent rich region moves (or, the oil-vacuum interface at desorption). They can be located with good accuracy, comparison with the theory is very simple, and gives us the two constants D_o and α, which describe the concentration dependent diffusivity at small values of ϕ.

1.4. Present Experiments and Literature

Ghanavati et al [18] have provided a review on a lot of data that have been reported on diffusivities of solvents in crude oil. The reasons why the results cannot be used or are not relevant to present purposes are varied and only some publications are described below. Guerrero et al [19] and Afshai and Kantzas [20] consistently fit their data to an expected profile using constant diffusivity. They also neglect the convective term, assume no swelling, and interpolate to get diffusivity as a function of concentrations, using spatially averaged concentration in the unsteady state case as the above concentration. As mentioned earlier, we are aware that all these assumptions produce errors, although, it is not clear by how much. Both our formulation and experiments avoid these problems. Fadei, Shaw and Swinton [21] actually measure the concentration profile when heavy oil is contacted with toluene over microscopic

distances. They do not include convection, and back calculate the diffusivity from the partial differential equation that has no convective term, and use mass fractions. They use light absorption to calculate the solvent concentration but cannot process deep into the oil side because it is all black there. Their results range from toluene mass fraction of 0.1 to 0.9 and diffusivities of 0.5×10^{-5} to 3×10^{-5} cm^2/s. The diffusivity values are quite high and concentrations do not approach zero concentration well. Similar results are seen for pentane in heavy oil [22] where x-ray absorption is used instead of visible light. The diffusion data as a function of mass fraction of pentane are concave upwards instead of convex upwards as in case of toluene. In the VAPEX process the solvent enters the region occupied by heavy oil and the leading edge is at zero solvent concentration. This is where the diffusion coefficient is expected to be the lowest and would control the rate of penetration into the oil.

The present scheme takes into account that it is very difficult to see inside black oil and utilizes the fact that the oil-solvent junction will be sharp. Vrentas and Duda [7] discuss diffusivity data of ethylbenzene in polystyrene that show that the diffusivities fall from 5×10^{-7} to 10^{-9} cm^2/s when the solvent concentration falls from 0.1 mass fraction to zero. The lowest diffusivity found in the above experiments is 10^{-7} cm^2/s by Afshai and Kantzas [20]. It is reasonable to suggested that the diffusivity of a solvent in heavy oil behaves in the same way as that in dry polymer. It has been observed earlier that the properties of heavy oil-solvent system follows the free volume model [11] and the free volume theory predicts the sharp fall in diffusivities at low concentrations. Strong concentration dependence at low solvent concentrations implies a very large concentration sharpening as seen in Fig. 1(c). The details of the above development in form of solution Eqs. (1) and (8) for large values of α are given in Appendix A. The experiments below where a liquid solvent is layered on the heavy oil and the interface is tracked with time, provides a very simple way to obtain concentration dependent diffusivities because the solution to the boundary value problem is known. Because the encroaching solvent front is led by a region of very low solvent concentration, it is this speed that is rate controlling. We can hence simplify measurements by tracking the speed of the front and not the concentration distribution in boundary layer. This novel method is attempted below for the first time. The dissolution experiments give us one number for two constants D_o and α and it is expected that a desorption experiment will provide another number allowing us to calculate the two constants. Because the nature of heavy oil and solvent are not accounted for, the D_o and α

pair are unique to a solvent-heavy oil pair. For completion, it is noted that as the free volume becomes large at large solvent volume fractions ϕ, Eq. (1) is not valid there.

Most of these studies are based on numerical solutions. Because of the strong concentration dependence on diffusivity, the solution is expected to change very steeply in some region. In fact, the limit $\varepsilon \to 0$, we get a discontinuous solution to Eq. (A-1) in the Appendix, with an infinite concentration gradient at the front. It implies that the error in discretization in terms of Δx can be kept small, nevertheless the error in $\Delta\phi$ will be large because the concentration gradient is so steep. Further computations are required to locate the interface and the results compared to experiments. This has to be done iteratively. Thus, when α is large, we have lengthy and difficult set of computations before us. In contrast, the asymptotic schemes used here is focused on keeping the error within bounds, here of the order less than $1/(\alpha\phi_\infty)$ and probably $1/(\alpha\phi_\infty)^2$.

2. Experimental

Heavy oil from A Hauser, Kansas, was used below. Brookfield viscometer was used to measure the viscosity of 4253 mPa.s (cp) at room temperature (~ 23ºC) and API gravity was found to be 19.9º (specific gravity of 0.934) and 929.8 mPa.s at 50 ºC and an API gravity of 21.9º (sp.gr. 0.9224). See Table 1. Solvents, *n*-hexane, *n*-heptane and toluene were purchased from Sigma Aldrich and used as received.

Table. 1: Properties of oil.

	Room temperature (23ºC)	30ºC	40ºC	50ºC
Viscosity mPa.s (cp)	4253	1884	1206	929.8
API gravityº/sp.gr	19.9º/0.9340			21.9º/0.9224

Oil was first preheated to 90 ºC in a water bath and then poured into a test tube in the water bath as oil at 90 ºC flowed more easily. The test tube was held in a metal holder in the water bath which was checked to be vertical. The bath temperature was then brought down to 30 ºC. Solvent, preheated to 30 ºC was then very gently poured on the oil when it reached 30 ºC. We

have performed such experiments earlier where one aqueous solution was contacted with another or with a low viscosity oil, where the layering process was very difficult. The upper liquid was layered over the lower liquid over a long time using a micropipette [23]. However, it was much easier here because the heavy oil is very viscous and damped disturbances well. Only a metered pipette was used to layer the top liquid on the glass walls to dampen the flow. Upon addition of solvent on oil, the solvent appeared to be immiscible with the oil and an interface was formed which remained clear and easy to track as seen in Fig. 2(a). The initial height of the solvent interface was noted and the test tube was sealed. Every hour the test tube was removed from the water bath and a photograph taken. Fig. 2(a) shows a series of photographs of a same system. Individual photographs were enlarged as shown in Fig. 2(b) for hexane on oil at 30 ºC at 4 hours. The curvature observed in the oil profiles is in large part due to the curvature of the glass tube of 10.99 mm inside diameter. The interfacial region was obtained by scanning horizontally from top and going down until a position was found that was all black over the full cross-section: that is the lower line in 2(b). Another attempt was stopped where the color was not black over the entire cross-section. The difference was 0.4 mm and hence the mathematical interface located midway had an error of ± 0.2 mm. The errors were determined for each case. The two lines in 2(b) were cut in half to aid viewing. With care, the error can be halved to ± 0.1 mm, but not always. It is noteworthy that this is the slice where Fadei, Shaw and Swinton [21] had measured the concentration profile of the solvent. On the other hand, in dissolution of solid polymers, this slice is compressed into a surface [4]. This is also the procedure here, but we also make certain that conservation of species is not violated. Nevertheless, we cannot locate such an interface experimentally except with an error that due to concentration sharpening is very small.

Measurements were discontinued in 3-4 hours. At 5 hours, the interfacial region became quite fuzzy and the bath temperature allowed to return to room temperature. Pictures were taken 24 and 48 hours later as shown, where the solution was fully equilibrated. At 48 hours, the liquid was drained out and showed the asphaltene precipitate adhering to the sides. All of the above description covers the full panel of photographs in Fig. 2(a).

These experiments were carried out for hexane, heptane and toluene at 30º, 40º and 50 ºC. Toluene becomes dark too easily at higher temperatures. Although we took care to satisfy the accuracy maintained here, the error in this case is expected to be more. One other system that

was analyzed, was 80 vol.% oil and 20 vol.% heptane (or hexane) which was contacted with heptane (or hexane) at 50 ºC.

(a)

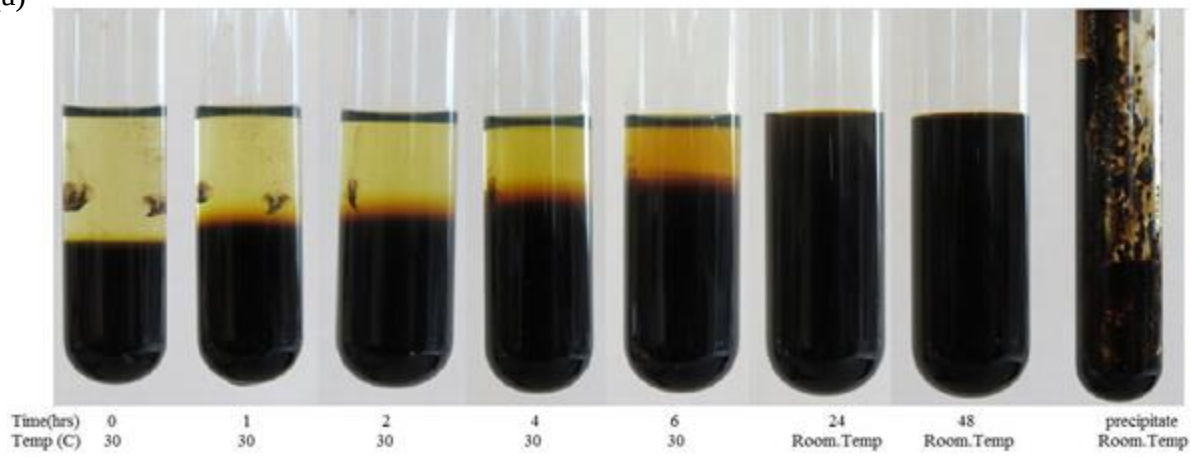

(b)

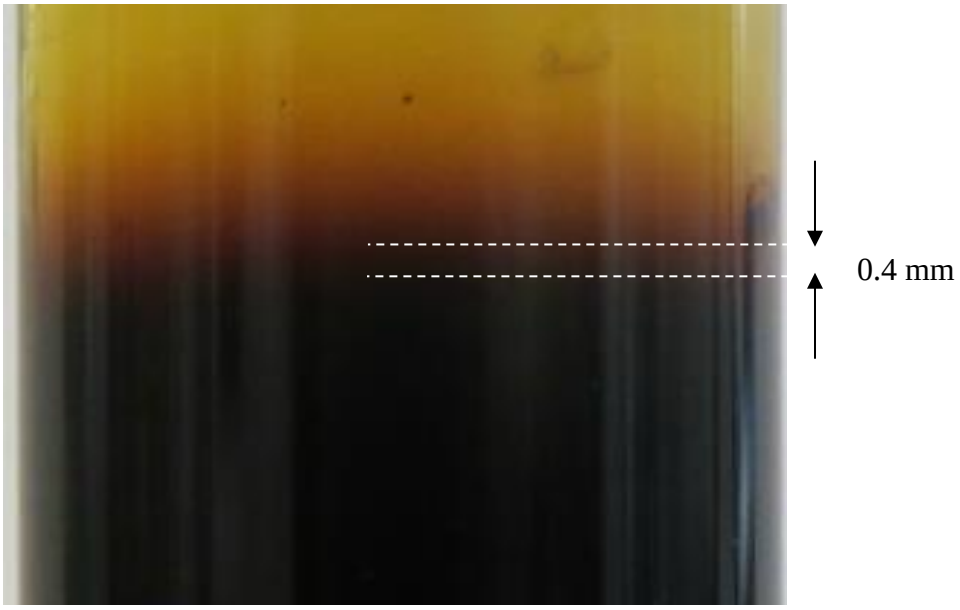

Fig. 2: (a) Interface between heavy oil and solvent, hexane, from 0 to 4 hours at 30 ^{o}C. Solvent interface height decreases with time. The sample was allowed to rest for 48 hours at room temperature and diluted oil was poured out to reveal asphaltene precipitation on the sides of the test tube. (b) Enlarged portion from a heavy oil-hexane sample at 4 hours showing the interfacial region. Interface is not of zero thickness, but about 0.4 mm thick.

Desorption experiments were very difficult to carry out. First of all, it made no difference if a vacuum was pulled over the mixture or if the mixture was allowed to evaporate in air. It suggests that the mass transfer resistance in the liquid phase was just too high that the two cases gave the same result, which is that the solvent concentration at the interface is always zero. Secondly, desorption was very slow, so much that for initial solvent volume fraction of 0.2, there was no change in the level even in 2-3 days. As a result, we turned to initial solvent volume fractions of 0.5 and 0.6. Even there, desorption was very slow for heptane and toluene so that only the experiments at high temperature, 50 ºC were conducted. Since hexane was more volatile, desorption experiments were studied at the lower temperatures of 30 and 40 ºC as well. Further, to stop the oil from clinging to the sides as the interface receded, we rinsed the inside of the tube with polydimethyl siloxane first, which made the walls non-wetting to oil. Finally, in spite of all these steps, the interface looked slightly bowed. The numbers for the liquid level were all collected at the center of the tube where the interface was the lowest.

3. Results and Discussion

The viscosities and some specific gravities are shown in Table 1. The heights of the interfaces with time for the three solvents are shown in Fig. 3(a) and the changes in the location of the interfaces with square root of time are shown in Fig. 3(b). The linear fits are very good. To determine the effect of temperature on the decrease of solvent interface height with time, dissolution experiments of heavy oil in hexane, heptane and toluene were performed at two higher temperatures, 40 and 50^{o}C. The changes in the interface height at 30, 40 and 50 ^{o}C with square root of time are shown in Fig. 4 (a) for hexane, 4(b) for heptane and 4(c) for toluene. Toluene-oil sample turned too dark after 2 to 3 hours at higher temperatures, but the fits are linear and agree well with Eq. (10) even for shorter time intervals. Asphaltene is insoluble in hexane, heptane but soluble in toluene [24, 25]. Dissolution of solvents in heavy oil led to asphaltene precipitation in hexane and heptane in present experiments but not in toluene.

Shown in Fig. 5 are the responses of hexane and heptane at 50 ºC where the oil phase initially had solvents at ϕ_o = 0.2. If we take the slope from Fig. 5 for hexane and heptane and divided with the slope for hexane and heptane when there is no solvent in oil present initially, we get 0.006/0.0049 = 1.22448 for hexane and 0.0043/0.0039 = 1.10256 for heptane. This ratio can

be calculated from Eqs. (9) and (10) to be 1.11803. The accumulated errors are 9% and 2.3% and show that the data and theory to be consistent and reliable to a high degree.

Desorption results are shown in Fig. 6 at 50 ºC for ϕ_o = 0.5 and 0.6 for hexane in 6(a), heptane in 6(b) and toluene in 6(c). The slopes and what they represent are shown in Table 2 which has all our data. Many entries under desorption are missing which shows our limited ability to perform experiments of this kind. Nevertheless, we were able to check if the manner in which we make the samples had an effect. Between one dissolution data and one desorption data, at the same temperature and solvent, it should be possible to calculate D_o and α, but we were unable to obtain reasonable values of the parameters, even though all we need are slopes at small times. As discussed later, the problem lies in our inability to do desorption studies at small dilutions.

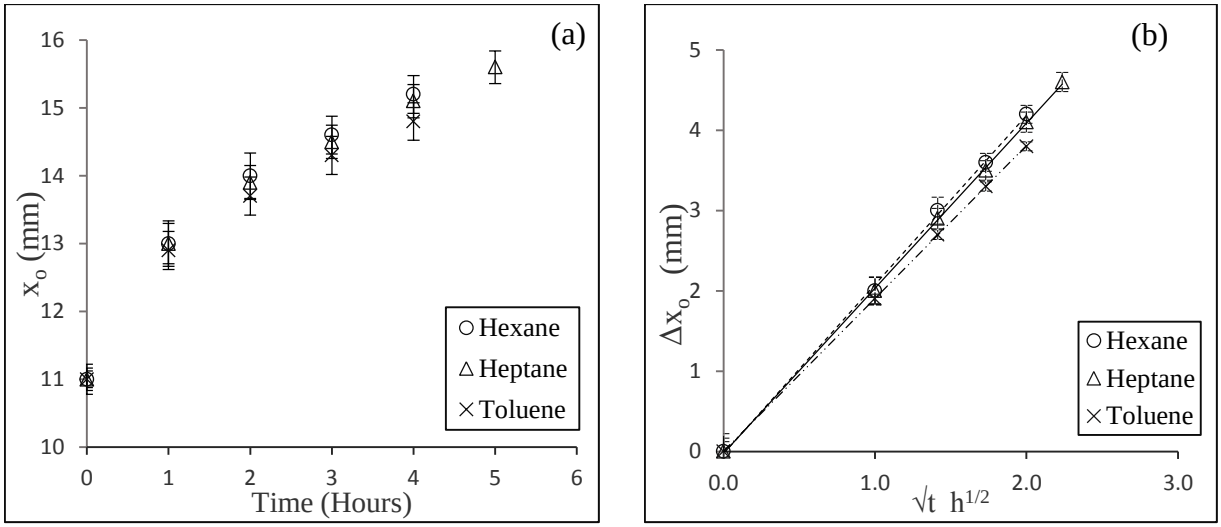

Fig. 3: (a) Location of the oil-solvent interface in dissolution of oil measured from the bottom, shown for hexane, heptane and toluene in heavy oil from 0 to 5 hours at 30 ^{o}C plotted as a function of time in hours. Error bars are shown. (b) Experimental data fitted to theory in form of location of the interface for hexane, heptane and toluene in heavy oil at 30 ^{o}C plotted versus $\sqrt{t}$ where time t is in hours. Error bars are shown. Circle for hexane, triangle for heptane and cross for toluene.

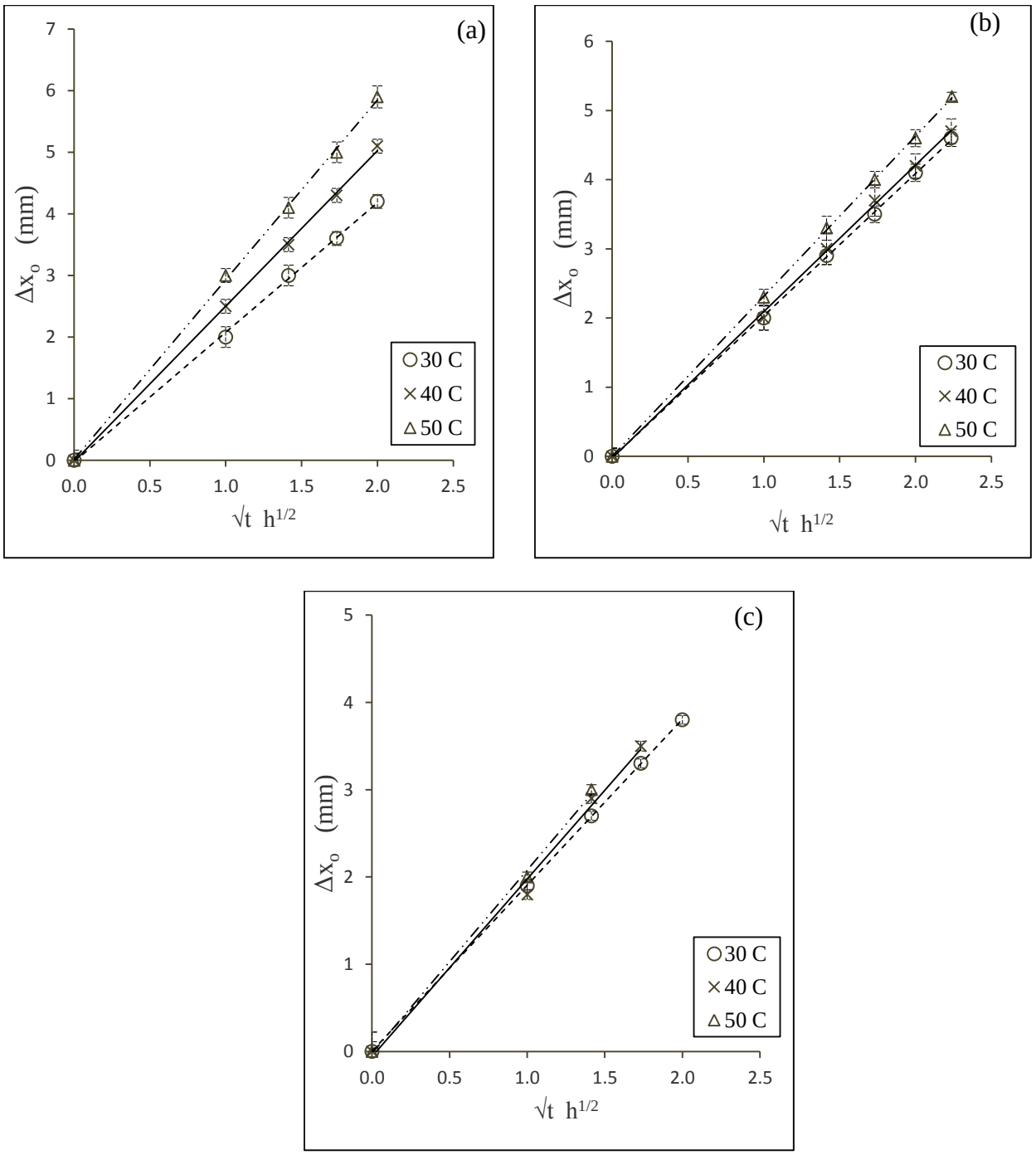

Fig. 4: (a) Experimental data fitted to theory in form of movement of the interface versus $\sqrt{t}$ are shown (a) at 30º, 40º and 50 ºC for hexane, (b) at 30º, 40º and 50 ºC for heptane and (c) 30º, 40 º and 50 ºC for toluene.

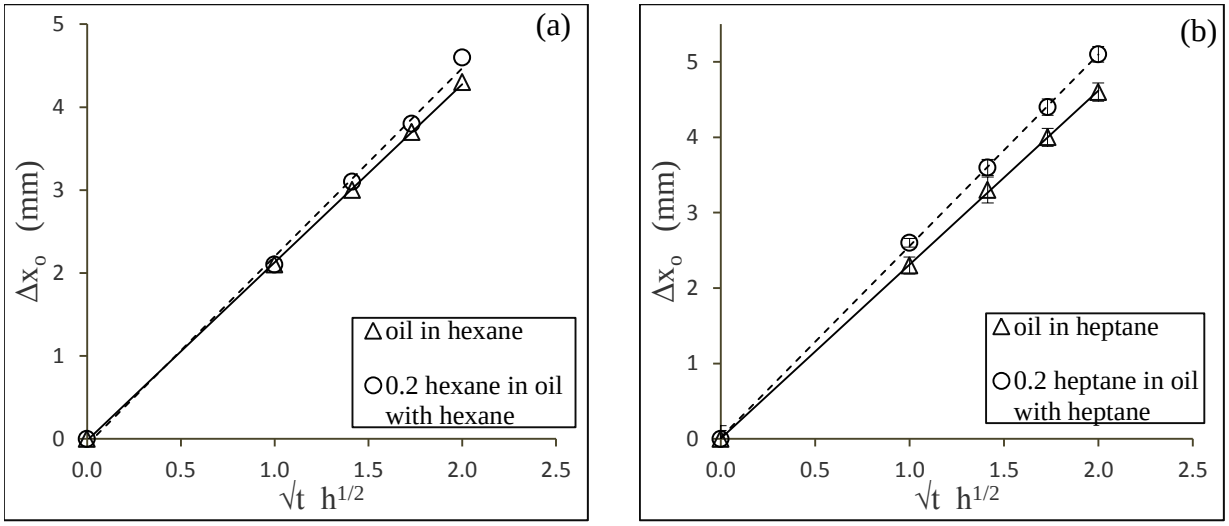

Fig. 5: Experimental data fitted to theory in form of movement of the interface in dissolution of oil for (a) pure oil in hexane and oil with 0.2 volume fraction hexane dissolving in pure hexane, and (b) pure oil in heptane and oil with 0.2 volume fraction heptane dissolving in pure heptane, both at 50 ºC.

Table. 2: Summary of the slopes (from Figs 3(b), 4, 5 for dissolution and Fig. 6 for desorption) from the data and their theoretical interpretation, Eqs. (11) and (13).

ϕ_o	Temp	Dissolution		Desorption	
		0.0	0.2	0.5 (A)	0.6 (B)
n-hexane	30 ºC	3.5×10^{-3}		1.6×10^{-3}	1.7×10^{-3}
	40 ºC	4.2×10^{-3}		1.9×10^{-3}	1.9×10^{-3}
	50 ºC	4.9×10^{-3}	5.9×10^{-3}	3.6×10^{-3}	3.7×10^{-3}
n-heptane	30 ºC	3.4×10^{-3}			
	40 ºC	3.5×10^{-3}			
	50 ºC	3.9×10^{-3}	4.3×10^{-3}	7.6×10^{-4}	7.6×10^{-4}
Toluene	30 ºC	3.2×10^{-3}			
	40 ºC	3.3×10^{-3}			
	50 ºC	3.5×10^{-3}		4.6×10^{-4}	4.6×10^{-4}

(A) Solvent added to oil to bring the solvent content to 0.5 volume fraction before desorption

(B) Solvent added to oil to bring solvent content to first 0.2 and homogenized and then more was added to bring it up to 0.6 before desorption

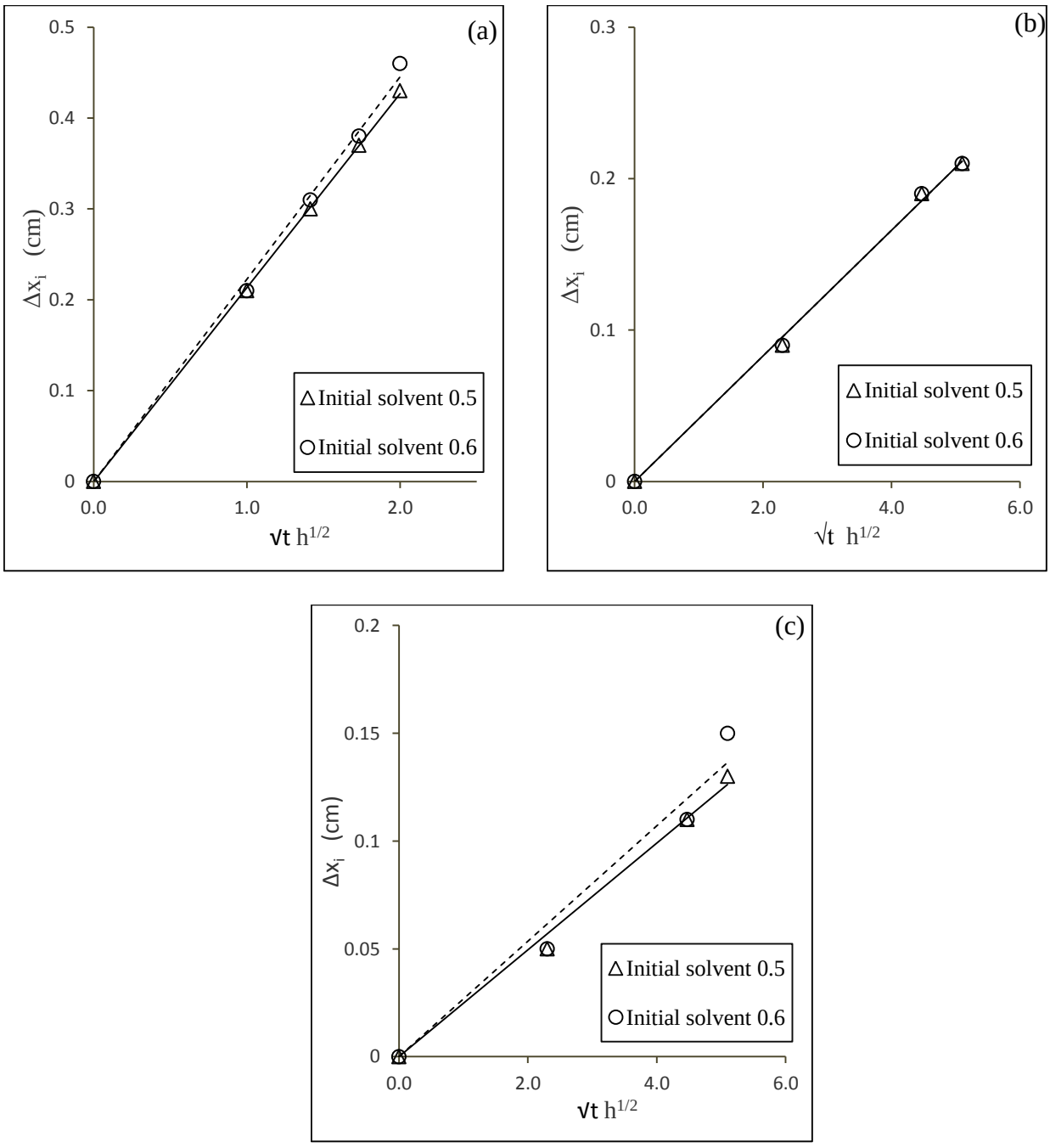

Fig. 6: Experimental data fitted to theory for desorption at 50 ºC of (a) oil with 0.5 and 0.6 volume fraction hexane (b) oil with 0.5 and 0.6 volume fraction heptane and (c) oil with 0.5 and 0.6 volume fraction toluene.

The diffusivity at infinite dilution can be calculated from Stokes-Einstein equation

$$D_o^{SE} = \frac{k_B T}{6\pi\mu_o a} \tag{14}$$

where k_B is the Boltzmann constant, μ_o is viscosity of the uncontaminated oil, and a is the radius of the solvent molecule which can be taken to be half of σ from Lennard-Jones potential [16]. The calculated values of D_o using Stokes-Einstein equation are shown in Table 3. Vrentas and Duda [7] indicate that over the temperature ranges used here, the diffusivities of ethylbenzene in polystyrene at infinite dilution are at least as low as those in Table 3. It is now possible to combine Stokes-Einstein values for D_o, Table 3, with the values of the slopes (and their mathematical expressions) in Table 2, to calculate the values of α. These are shown in Table 4. It is seen that α values for dissolution are of the order of about 9 to 10. They decrease a little with increase in temperature, and do not change with the two cases of varying initial solvent concentrations in oil, volume fractions of 0.0 and 0.2. The values of α in desorption are about 4 to 9, that is, do not agree with the dissolution values. However, the results from the two initial concentrations appear to agree. In general, α is independent of initial solvent concentrations and its values do show this feature. The experimental errors translate to ± 0.1 for α in dissolution at 95% confidence level except in case of toluene where it goes up to ± 0.5 to ± 1.5.

Table. 3: Stokes-Einstein values for D_o Eq. (14).

T (^{o}C)	Temp (K)	Oil viscosity (g/cm·s)	Diffusivity (cm^2/s)		
			n-hexane	n-heptane	toluene
30	303.15	18.84	3.77 x10^{-9}	3.54 x10^{-9}	3.98 x10^{-9}
40	313.15	12.06	6.08 x10^{-9}	5.71 x10^{-9}	6.43 x10^{-9}
50	323.15	9.298	8.13 x10^{-9}	7.65 x10^{-9}	8.60 x10^{-9}

The fact that a dissolution-desorption pairs in Table 2 do not give acceptable values of the parameters most probably lies with high solvent concentrations used in the desorption studies. The free volume theory works only when the free volumes are low and restrict mobility.

Heavy oil just about falls in this region in its free volumes. In presence of large amount of solvent, the free volume will become large will not be rate controlling and the free volume theory will not work. However, we could not run desorption experiments in the region of low values of ϕ_o.

Table. 4: α values on combining data from Tables 2 and 3.

ϕ_o	Temp	Dissolution		Desorption	
		0.0	0.2	0.5 (A)	0.6 (B)
n-hexane	30 °C	9.6669 ± 0.12		8.8552 ± 1.50	7.1098 ± 1.11
	40 °C	9.5379 ± 0.10		8.5194 ± 0.24	6.9374 ± 0.72
	50 °C	9.5370 ± 0.10	9.7276 ± 0.13	9.6349 ± 0.05	7.7941 ± 0.18
n-heptane	30 °C	9.6832 ± 0.05			
	40 °C	9.2174 ± 0.09			
	50 °C	9.0895 ± 0.03	9.0470 ± 0.07	5.9999 ± 0.29	4.6450 ± 0.24
Toluene	30 °C	9.3793 ± 0.01			
	40 °C	8.9929 ± 0.54			
	50 °C	8.7342 ± 1.46		4.6884 ± 0.51	3.7415 ± 1.14

(A) Solvent added to oil to bring the solvent content to 0.5 volume fraction before desorption

(B) Solvent added to oil to bring solvent content to first 0.2 and homogenized and then more was added to bring it up to 0.6 before desorption

Since we have used a very low value of diffusivity at infinite dilution using Stokes-Einstein equation in desorption in particular, it would imply that it is correct if an average diffusivity $\bar{D}$ can be calculated for the desorption case. The rate at which the interface recedes is a moving boundary problem and a special case is that considered by Crank [26] and given in Appendix B. The result for desorption is

$$\Delta x_i = \frac{-2\phi_o e^{-\frac{\left(\Delta x_i / t^{1/2}\right)^2}{4D_o}} \left(\frac{\bar{D}t}{\pi}\right)^{1/2}}{\lambda\left(1+erf\left(\frac{\Delta x_i / t^{1/2}}{(4\bar{D})^{1/2}}\right)\right)} \qquad (15)$$

where $\lambda = \rho_o.v_o$, the density of oil ρ_o is interpolated from Table 1, and v_o the specific volumes of the solvents as functions of temperature are available in many data bases. Eq. (15) also shows that $\Delta x_i \propto t^{1/2}$. Values of the proportionality constants from the experimental data (slopes p) are taken from Table 2 and fitted to Eq. (15). (If we take $\Delta x_i / t^{1/2} = p$, then from Eq. (15) we get

$$p = \frac{-2\phi_o e^{-\frac{p^2}{4D_o}} \left(\frac{\bar{D}}{\pi}\right)^{1/2}}{\lambda\left(1+erf\left(\frac{p}{(4\bar{D})^{1/2}}\right)\right)}$$

. These are solved to get $\bar{D}$ which are shown in Table 5. They are low compared to all the diffusivity data from previous work discussed earlier. This reinforces our basic premise that the diffusivities start from very low values at infinite dilution.

Table. 5: $\bar{D}$ calculated using Eq. (15).

		Desorption $\bar{D}$ cm^2/s	
ϕ_o	Temp	0.5 (A)	0.6 (B)
n-hexane	30 ^{o}C	3.05 x10^{-6}	3.10 x10^{-6}
	40 ^{o}C	6.00 x10^{-6}	6.00 x10^{-6}
	50 ^{o}C	9.70 x10^{-6}	9.70 x10^{-6}
n-heptane	30 ^{o}C		
	40 ^{o}C		
	50 ^{o}C	6.00 x10^{-7}	6.00 x10^{-7}
Toluene	30 ^{o}C		
	40 ^{o}C		
	50 ^{o}C	5.00 x10^{-7}	5.00 x10^{-7}

(A) Solvent added to oil to bring the solvent content to 0.5 volume fraction before desorption

(B) Solvent added to oil to bring solvent content to first 0.2 and homogenized and then more was added to bring it up to 0.6 before desorption

Overall, it appears that the diffusivity of these solvents is strongly concentration dependent, and in particular follows Eq. (1). However, we encountered a problem that desorption was the experimental method of choice for determining in particular the diffusivity at infinite dilution. It only worked partially, although it showed that the assumed concentration dependence was correct. It is possible to measure diffusivity at infinite dilution separately [27], but it requires a

separate system and has not been attempted here. We have not found any effect on diffusion from asphaltene precipitation and have inferred that asphaltenes take over a day to precipitate.

The large concentration dependence of the diffusivity has two implications. The first is that although we can perform oil recovery simulations using an effective constant diffusivity, in practice this effective value is very difficult to determine [28]. Second, complications result when numerical simulations are carried out using a strongly concentration dependent diffusivity. It is prone to significant errors and stability problems [29].

4. Conclusions

The present method of measuring concentration dependent diffusivity is new and and is shown to work well. They are also consistent and accurate, showing good match with theory. However, it is not possible to get adequate data on desorption because of which either correlations have to be used for diffusivity at infinite dilution or other experiments need to be conducted to obtain this quantity. The data however show diffusivity to be strongly concentration dependent and the strong exponential dependence used here to be very suitable.

5. Appendix A

The derivations follow Neogi [6] where a finite system has been changed to an infinite one.

5.1. Dissolution

The development is based on the fact that the quantity ε, to be defined later, is small and hence $\ln\left|\frac{1}{\varepsilon}\right|$ is large but not very large. In particular, as $\varepsilon \to 0,\ \ln\left|\frac{1}{\varepsilon}\right| \to \infty$ but $\varepsilon^{v}\ln\left|\frac{1}{\varepsilon}\right| \to 0$ for all values of $v > 0$. Eq. (8) can be written as

$$\frac{\partial\theta}{\partial\tau} = \frac{\partial}{\partial x} e^{\bar{\alpha}\theta} \frac{\partial\theta}{\partial x} \qquad \text{(A-1)}$$

where as $x \to -\infty, \theta \to 0$ and as $x \to +\infty, \theta \to 1$. Here $\theta = \phi / \phi_\infty$, $\tau = tD_o$ and $\bar{\alpha} = \alpha\phi_\infty$. Substituting $\bar{\alpha} = \ln\left|\frac{1}{\varepsilon}\right|, X = \frac{x - x_o(\tau)}{\omega}, \theta \sim \left[\ln\left|\frac{1}{\varepsilon}\right|\right]^{-1} \theta_o + \ldots$ we get

$$\frac{d\theta_o}{dX}.(-\omega).\frac{dx_o}{d\tau} = \frac{d}{dX}[e^{\theta_o}\frac{d\theta_o}{dX}] \tag{A-2}$$

Eq. (A-2) is rewritten as

$$\frac{1}{1-A}\frac{d\theta_o}{dX} = \frac{d}{dX}[e^{\theta_o}\frac{d\theta_o}{dX}] \tag{A-3}$$

and

$$\frac{1}{1-A} = -\omega.\frac{dx_o}{d\tau} \tag{A-4}$$

where A is a constant. Here ω is small and goes to zero as $\varepsilon \to 0$. Eq. (A-3) can be integrated twice subject to the boundary conditions $X \to -\infty, \theta_o \to 0, \frac{d\theta_o}{dX} \to 0$ to get

$$\frac{1}{x_o(0) - x_o(\tau)}.X = Ei(\theta_o) \tag{A-5}$$

where the condition $X \to +\infty, \theta \to 1$ is met approximately. *Ei* is the exponential integral, a special function. The rate law in Eq. (A-4) now integrates to give

$$[x_o(0) - x_o]^2 = 2\tau / \omega \tag{A-6}$$

Now, the place where ω is introduced after Eq. (A-1) shows ω to be thickness of the profile where θ falls rapidly from 1 to zero. Eq. (A-4) also shows τ to be of the order of ω. So if we choose ω to be very small such as ε, then the profile falls very sharply, but stays for a very short time, which does not occur in practice. Thus, we increase the ω to be $\varepsilon \ln\left|\frac{1}{\varepsilon}\right|$ using the function of ε encountered earlier.

It is now possible to define x_o as equivalent to $\phi = 0$ for $x < x_o$ and $\phi = \phi_\infty$ for $x \geq x_o$. It leads to a conservation rule that

$$\int_{x_o}^{\infty} (\phi - \phi_\infty) dx = 0 \tag{A-7}$$

Differentiating Eq. (A-7) with τ, using Eq. (A-1) and boundary conditions,

$$\frac{d}{d\tau}[x_o(0) - x_o(\tau)] = e^{\ln\frac{1}{\varepsilon}.\theta} . \frac{\partial \theta}{\partial x}\bigg|_{x=x_o} \tag{A-8}$$

then using Eq. (A-5), Eq. (A-6) is obtained. In dimensional form, Eq. (A-6) is

$$\Delta x_o = [\frac{2D_o e^{\alpha\phi_\infty} t}{\alpha\phi_\infty}]^{1/2} \tag{A-9}$$

and Eq. (A-9) is Eq. (9) in the text.

5.2. Desorption

In case of desorption set $\theta = 1 - \bar{\theta}$ in Eq. (A-1), resulting in

$$\frac{\partial \bar{\theta}}{\partial \tau} = \frac{\partial}{\partial x} e^{\ln\frac{1}{\varepsilon}} . e^{-\ln\frac{1}{\varepsilon}.\bar{\theta}} \frac{\partial \bar{\theta}}{\partial x} \tag{A-10}$$

or

$$\frac{\partial \bar{\theta}}{\partial \tau} = \frac{1}{\varepsilon} \frac{\partial}{\partial x} e^{-\ln\frac{1}{\varepsilon}.\bar{\theta}} \frac{\partial \bar{\theta}}{\partial x} \tag{A-11}$$

where as $x \to -\infty, \bar{\theta} \to 0$ and as $x \to +\infty, \bar{\theta} \to 1$. Note for future reference, an extra ε on the right hand side in Eq. (A-11). With $\hat{\alpha} = \alpha\phi_o = \ln\left|\frac{1}{\varepsilon}\right|, X = \frac{x - x_o(\tau)}{\omega}, \bar{\theta} \sim \left[\ln\left|\frac{1}{\varepsilon}\right|\right]^{-1} \theta_o + \ldots$ and using the same procedure as above,

$$\frac{1}{x_o(0) - x_o(\tau)} . X = E_1(\theta_o) \tag{A-12}$$

$$[x_o(0) - x_o]^2 = 2\tau / (\varepsilon\omega) \tag{A-13}$$

Eq. (A-13) in dimensional form is given in Eq. (12). Note that in Neogi [6], the extra ε is moved to the profile Eq. (A-12) and the rate law Eq. (A-13) is consequently modified. However, that makes the change in the concentration in the profile less steep. As a result, the ε has been moved to the rate law and, the time over which Eq. (A-13) applies is considerably shortened. that is, τ is of the order of $\varepsilon\omega = \varepsilon^2 \ln\left|\frac{1}{\varepsilon}\right|$. Other possible forms for ω could not be used.

It is possible to see in Eq. (A-1) that in the limit when $\varepsilon \to 0$, $\partial\theta / \partial x \to 0$. It produces a discontinuous profile when it jumps from $\theta = 0$ to $\theta = 1$ at some point inside leading to infinite gradient there. Thus it is a singular perturbation problem. The asymptotic expansion obtained here is the one that straddles the interface with an error smaller than $1/(\alpha\phi_\infty)$ or in terms of perturbation expansions $\sim o\left[\ln\left|\frac{1}{\varepsilon}\right|\right]^{-1}$, probably of $1/(\alpha\phi_\infty)^2 \sim O\left[\ln\left|\frac{1}{\varepsilon}\right|\right]^{-2}$ which is quite small. Two other asymptotic expansions are needed about $\theta = 0$ to $\theta = 1$ and matched. However, only the part useful for application, has been accounted for. In fact knowing that $\alpha = B_d(g - f)/f^2$ in Eq. (4c) is the large quantity, the presents result will remain unchanged even if one starts with the full form of diffusivity given in Eq. (4b).

6. Appendix B

The derivation below follows Crank [26]. The governing equation, Eq. (8) becomes

$$\frac{\partial\phi}{\partial t} = \bar{D}\frac{\partial^2\phi}{\partial x^2} \tag{B-1}$$

Subject to the boundary conditions that as $x \to -\infty$, $\phi \to \phi_o$ and at $x = x_o$ $\phi = 0$. The jump mass balance is $\dot{m} = \rho(0 - \frac{dx_o}{dt}) = c(0 - \frac{dx_o}{dt}) - \bar{D}\frac{\partial c}{\partial x}$ at the interface. Here $\dot{m}$ is the solvent transferred across the interface (since oil is non-volatile), and ρ is the total density at the interface. Since the solvent concentration at the interface is zero, $\rho = \rho_o$ the density of pure oil at that temperature.

The rest follows Crank [26] error functions solution and the boundary conditions yield both the constants of integration and the location of the boundary.

In desorption experiments, solvent was allowed to evaporate. The result for desorption is

$$\Delta x_i = \frac{-2\phi_o e^{-\frac{\left(\Delta x_i / \sqrt{t}\right)^2}{4D_o}} \left(\frac{D_o t}{\pi}\right)^{1/2}}{\lambda\left(1+erf\left(\frac{\Delta x_i / \sqrt{t}}{\sqrt{4D_o}}\right)\right)} \qquad \text{(B-2)}$$

where x_i here is the visible oil-vacuum interface and λ corresponds to the product of density of oil and specific volume of solvent. More importantly $\Delta x_i = -p\sqrt{t}$ where p is a constant. Eq. (B-2) is Eq. (15).

References

[1] D.K. Banerjee, Oil Sands, Heavy Oil and Bitumen From Recovery to Refinery, PennWell Corp, 2012, pp. 65.
[2] L. Lin L, F. Zeng, Y. Gu, J. Pet. Sci. Eng. 118 (2014) 27-39.
[3] J.M. Prausnitz, R.N. Lichtenthaler, and E.G. De Azevedo, Molecular Thermodynamics of Fluid Phase Equilibrium, Prentice -Hall, New Jersey, 3rd edition, 1999, pp. 607.
[4] B.A. Miller-Chou, and J.L. Koenig, Prog. Polymer Sci. 28 (2003) 1223-1270.
[5] J.S.Vrentas, and C.M. Vrentas, J. Polym. Sci. B Polym. Phys. 36 (1998) 2607 – 2614.
[6] P. Neogi, Chem. Eng. Comm. 68 (1988) 185-195.
[7] J.S.Vrentas, and J.L. Duda, AIChE J. 25 (1979) 1-24.
[8] M.H. Cohen and D. Turnbull J. Chem. Phys. 31(1959) 1164–1169.
[9] H. Sabbagh and B.C. Eu, Physica A. 389 (2010) 2325-2328.
[10] H. Fujita, Adv. Polym. Sci. 3 (1961) 1-47.
[11] T. Tran, P. Neogi, and B. Bai, Chem. Eng. Sci. 80 (2012) 100-108.
[12] F.T.H. Chung, R.A. Jones, and H.T. Nguyen, SPE Res. Eng. 3 (1988) 822 –828.
[13] S. Prager, and L.A. Long, J.Am.Chem. Soc. 73 (1951) 4072-4075.
[14] V.Mohan, P.Neogi and B.Bai, Can.J.Chem.Eng. 95(2017) 796-798.
[15] J. Camacho, and H. Brenner, IECRes. 34 (1995) 3326-3335.
[16] J.C. Slattery, Momentum, Energy and Mass Transfer in Continua, McGraw-Hill Book Co, New York , 2nd edition, 1972, pp.18.

[17] R.B. Bird, W.E. Stewart, and E.N. Lightfoot, Transport Phenomena, John Wiley, New York, 2nd edition, 2002, pp.536.
[18] M. Ghanavati, H. Hassanzadeh, and J. Abedi, Canad. J. Chem. Eng. 92 (2014) 1455-1466.
[19] U. Guerrero-Aconcha, D. Salama, and A. Kantzas, Diffusion coefficient of n-alkanes in heavy oil. Paper presented at 2008 SPE Ann. Tech. Conf., Denver Colorado, SPE 115346.
[20] B. Afsahi, and A. Kantzas, J. Canad. Pet. Tech. 46 (2007) 56-61.
[21] H. Fedai, J.M. Shaw, and D. Swinton, Energy & Fuels. 27 (2013) 2042-2048.
[22] X. Zhang, M. Fulem, and J.M. Shaw, J. Chem. Eng. Data. 52 (2007) 691-694.
[23] C.L. Williams, A.R. Bhakta, and P. Neogi, J. Phys.Chem.B. 102 (1999) 3242-3249.
[24] B. Guo, S. Song, A. Ghalambor, and T.R. Lin, Offshore Pipelines: Design, Installation and Maintenance, Elsevier, UK, 2nd edition, 2014 pp. 199.
[25] A. Nikolaides, Highway Engineering: Pavements, Material and Control of Quality. CRC Press, 2015, pp. 110.
[26] J. Crank, Free and Moving Boundary Problem, Oxford Science Pub., Oxford, 1984, pp. 102.
[27] E.L. Cussler, Diffusion Mass Transfer in Fluid Systems, Cambridge, 3rd edition, 2009, pp. 85.
[28] G.S. Park, Methods of measurements, in Diffusion in Polymers, J. Crank and G.S. Park, eds., Academic Press, New York, 1968, pp.1.
[29] W.F. Ames, Nonlinear Partial Differential Equations in Engineering, Academic Press, New York, 1965, pp. 320.